TECHNICAL PAPER

Influence of secondary phases in A356 MMCs on their mechanical properties at macro- and nanoscale

Aleksandar Vencl[1,2] · Ilija Bobić[3] · Miloš Stanković[4] · Pavol Hvizdoš[5] · Biljana Bobić[6] · Blaža Stojanović[7] · Friedrich Franek[8,9]

Abstract

Metal matrix composites are very inhomogeneous materials, and their properties depend on various parameters (production process, constituents, their interfaces, etc.). The influence of SiC microparticles (40 μm) reinforcement and graphite macroparticles (200–800 μm) addition on the mechanical properties of Al–Si A356 alloy, produced by compocasting, has been assessed using macro- and nanoscale measurements of hardness and modulus of elasticity. The Al makes over 90 wt% of the A356 alloy, so the nanoscale measurements were performed on different α phase regions on each material (core of α phase, eutectic α phase, and α phase near the phase boundaries α phase/secondary phases). The results showed that there is no direct correlation between mechanical properties on macro- and nanoscale. The nanoscale results also showed that the secondary phases (SiC and graphite particles) can have significant effect on the mechanical properties on the atomic level, i.e. in the α phase regions very close to the secondary phases.

Keywords A356 alloy · Hybrid composites · Compocasting · SiC · Graphite · Hardness · Modulus of elasticity

1 Introduction

The A356 alloy is a hypoeutectic Al–Si alloy with a small amount of magnesium. It belongs to a group of casting alloys. The mechanical properties of the alloy can be

Technical Editor: Izabel Fernanda Machado, Dr.

✉ Aleksandar Vencl
avencl@mas.bg.ac.rs

Ilija Bobić
ilijab@vinca.rs

Miloš Stanković
mstankovic@mas.bg.ac.rs

Pavol Hvizdoš
phvizdos@saske.sk

Biljana Bobić
biljanabobic@gmail.com

Blaža Stojanović
blaza@kg.ac.rs

Friedrich Franek
friedrich.franek@tuwien.ac.at; friedrich.franek@ac2t.at

1 Faculty of Mechanical Engineering, University of Belgrade, Kraljice Marije 16, Belgrade 35 11120, Serbia

2 South Ural State University, Lenin prospekt 76, Chelyabinsk, Russia 454080

3 Institute of Nuclear Sciences "Vinca", University of Belgrade, Mike Petrovića Alasa 12-14, Belgrade 11001, Serbia

4 Innovation Center of the Faculty of Mechanical Engineering in Belgrade, Kraljice Marije 16, Belgrade 35 11120, Serbia

5 Institute of Materials Research, Slovak Academy of Sciences, Watsonova 47, 04001 Košice, Slovakia

6 Institute of Chemistry, Technology and Metallurgy, University of Belgrade, Njegoševa 12, Belgrade 11000, Serbia

7 Faculty of Engineering, University of Kragujevac, Sestre Janjić 6, Kragujevac 34000, Serbia

8 Institute of Engineering Design and Logistics Engineering, TU Wien, Getreidemarkt 9/E307, 1060 Vienna, Austria

9 AC²T research GmbH, Excellence Centre of Tribology, Viktor-Kaplan-Str. 2/C, 2700 Wiener Neustadt, Austria

improved by the appropriate heat treatment (especially using the T6 regime). Due to a good combination of mechanical and physical properties, and high corrosion resistance, the A356 alloy is commonly used in the automotive and aircraft industry. The alloy solidifies in a relatively wide temperature range (615 to 555 °C) [1] and is suitable for semi-solid processing [2]. Mechanical properties of semi-solid products of the A356 alloy can also be improved by the appropriate heat treatment regime [3].

The properties of the A356 alloy can also be improved by adding hard ceramic particles and fibres (SiC, Al_2O_3, etc.) in the matrix alloy, using different casting techniques [4, 5]. In the compocasting method, under the influence of shear forces (due to mixing), the semi-solid melt of the matrix alloy behaves as pseudoplastic non-Newtonian fluid. The apparent viscosity of the melt can be optimised by controlling the mixing rate. As a result, a favourable distribution of added particles can be achieved [6]. Incorporation of the secondary phase during the compocasting process is carried out at a lower temperature than in the case of the production of composites through the liquid casting processes (e.g. Vortex method). This enables energy savings and the extended tool life [6], which reduces the production costs. The compocasting method is suitable for the production of conventional A356/SiC or A356/graphite composites, as well as hybrid A356/SiC/graphite composites [7–9].

It has been shown, in our previous study [9], that the structure of hybrid A356/SiC/graphite composites is very complex, with a large number of phase boundaries matrix/secondary phases, indicating that the interface in hybrid composites should be further studied. The main goal of this paper is to evaluate the influence of secondary phases (SiC and graphite) in the produced composites on their structural and mechanical properties. In order to achieve this goal, metallographic examinations were performed as well as the measurement of the modulus of elasticity and shear modulus at macroscale. Also, nanoindentation was carried out in α phase regions in the thixocasted A356 alloy and in produced composites, in order to determine the nanohardness and modulus of elasticity in these regions.

2 Experimental details

2.1 Materials

The hypoeutectic Al–Si alloy A356 (EN AlSi7Mg0.3), slightly modified with 0.03 wt% strontium (Sr), was used as the matrix material for obtaining composites. Strontium was added to the A356 alloy melt to modify the eutectic silicon particles. The matrix material, obtained by semi-solid processing (thixocasting), was used as a reference material (designated as A356 thixo). Composites were produced by

the compocasting process, using the silicon carbide (SiC) microparticles (average diameter 40 μm) and graphite (Gr) macroparticles (200–800 μm). The amount of incorporated silicon carbide was 10 wt%, while the amount of graphite was 1 and 3 wt%. The following three composite materials were obtained: A356 thixo + 10 wt% SiC (designated as A356–10SiC), A356 thixo + 10 wt% SiC + 1 wt% Gr (designated as A356–10SiC–1Gr), and A356 thixo + 10 wt% SiC + 3 wt% Gr (designated as A356–10SiC–3Gr).

Apparatus used for the semi-solid processing of matrix alloy and composites is described elsewhere [10]. Parameters of the thixocasting and compocasting process, for the purpose of comparison, were similar in production of A356 thixo and composites samples. Detailed description of the materials producing procedure is presented elsewhere [9]. All specimens were subjected to modified T6 heat treatment with the following parameters: solution heat treating at 540 °C for 4 h with water quenching and artificial ageing at 160 °C for 5 h with water quenching.

2.2 Macroscale characterisation

Determination of modulus of elasticity and shear modulus was performed on the non-destructive testing system Buzz-o-sonic Lab Kit 5.9 on specimens with dimensions $30 \times 15 \times 6$ mm, using the impulse excitation technique (according to ASTM E1876). This technique is also known as: Impulse excitation of vibration; Resonant vibration; Impact acoustic resonance; Ping test; and Eigen frequency method. A schematic diagram of impulse excitation technique testing is shown in Fig. 1.

The procedure of testing was as follows: a test specimen is tapped lightly with a impulser (flexible polymer rod with steel ball) causing a standing wave to be generated in the solid; the resulting vibration (sound) is captured by a non-contact transducer (microphone attached to a PC); the sound is analysed using a fast Fourier transform algorithm, and the fundamental resonant frequency is isolated and measured by the signal analyser. The modulus of elasticity and shear modulus are calculated from the known densities,
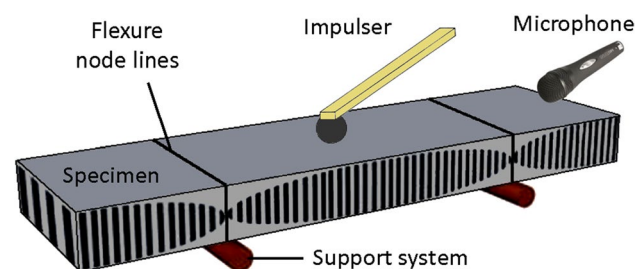
Fig. 1 A schematic diagram of impulse excitation technique testing (out-of-plane flexure)

dimensions and Poisson's ratios of the specimens and obtained fundamental resonant frequencies.

2.3 Nanoscale characterisation

Specimens for the nanoscale characterisation were prepared in a standard way applying grinding and polishing [9]. Nanoindentation tests of the produced materials included hardness and modulus of elasticity measurements. These tests were carried out on a nanomechanical test instrument TI 950 TriboIndenter, using instrumented indentation method (according to ISO 14577-1) under the assumption that all tested regions have Poisson's ratio of 0.33 [1]. The following indentation parameters were used to produce several multicycle indents on each sample: diamond Berkovich indenter (modulus of elasticity 1141 GPa, Poisson's ratio 0.07); ambient air; room temperature 22 °C; constant loading/unloading rate 2.5 mN/s; maximum load 5 mN; pause at maximum load 2 s; pause at unloaded condition 0 s; and number of cycles 10 cycles (Fig. 2a). With the multicycle mode, which is used in tests, indentation is repeated in the same place 10 times (cycles) producing one single indent. The measured values of the hardness and modulus of elasticity differed for each cycle (Fig. 2b), and the average values were calculated for each indent.

Nanoidentation measurements were performed on up to 5 different α phase regions on each material, i.e. core of α phase; α phase in eutectic; α phase near SiC particles; α phase near graphite particles; and α phase near SiC and graphite particles. Each region is measured on several locations (several indents), and the results for each material and region are averaged and presented. Distance between the individual indents in the same region was at least 12 μm. After the testing of each region, position of indents is recorded with the optical microscope (OM) image and with scanning probe microscope (SPM) image at higher magnification. The main purpose of these images was to show the position of the indents, although some were also used for the concise analysis of the obtained material microstructures.

3 Results and discussion

3.1 Macroscale properties

Macrohardness values of the A356 thixo alloy and the composites A356–10SiC, A356–10SiC–1Gr and A356–10SiC–3Gr [9] are shown in Table 1, together with the measured values of the modulus of elasticity and shear modulus. The mechanical properties of the thixocasted A356 alloy and the composites with the A356 alloy matrix can
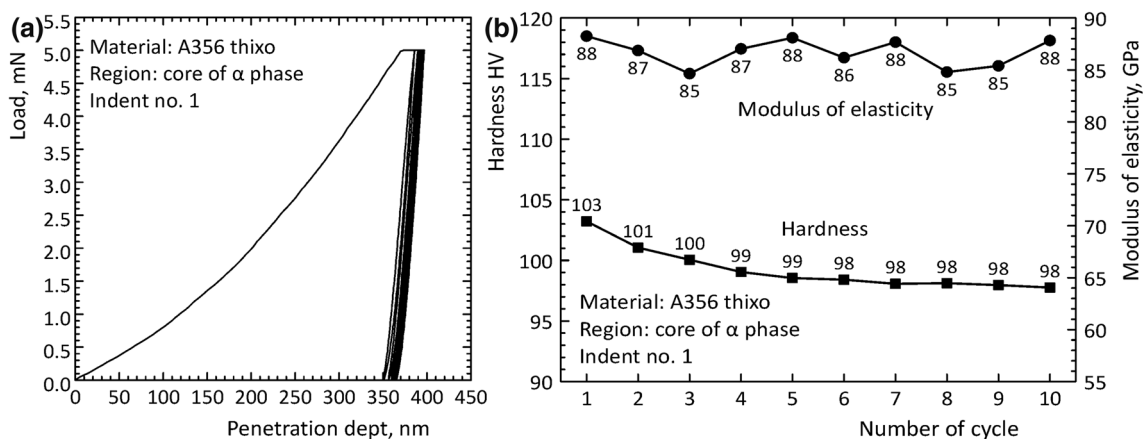
Fig. 2 Multicycle mode nanoindentation testing (typical shapes): **a** load versus penetration depth curve and **b** dependence of the measured values on number of cycles

Table 1 Macrohardness, modulus of elasticity and shear modulus of thixocasted A356 alloy and composites

Mechanical property	Material designation			
	A356 thixo	A356–10SiC	A356–10SiC–1Gr	A356–10SiC–3Gr
Macrohardness HV 5	69.5 (SD = 1.32)	72.0 (SD = 2.21)	76.5 (SD = 4.83)	77.0 (SD = 5.63)
Modulus of elasticity, GPa	65.0 (SD = 1.06)	79.8 (SD = 1.41)	71.9 (SD = 1.39)	56.3 (SD = 1.23)
Shear modulus, GPa	24.4 (SD = 0.40)	30.0 (SD = 0.53)	27.0 (SD = 0.52)	21.2 (SD = 0.46)

SD: standard deviation

be compared with the mechanical properties of the conventionally casted A356 alloy [1]. However, the morphological differences between the cast A356 alloy and the thixocast A356 alloy [9] should be considered.

Macrohardness value of the A356 thixo alloy (which is heat-treated according to the modified T6 regime) is very close to the typical hardness value of the sand-casted A356 alloy, heat-treated according to the conventional T6 regime (70 HB) [1]. The values of modulus of elasticity and shear modulus of the A356 thixo alloy are also slightly lower than the typical modulus of elasticity (72.4 GPa) and shear modulus (27.2 GPa) values of the conventionally casted and T6 heat-treated A356 alloy [1]. With the addition of SiC particles (composite A356–10SiC), there was a slight increase in hardness, but the values of the modulus of elasticity and shear modulus increased significantly (approx. 24%). In the case of hybrid composites (A356–10SiC–1Gr and A356–10SiC–3Gr), the hardness values were increased, while the values of the modulus of elasticity and shear modulus were reduced.

The mechanical properties of the cast A356 alloy depend on the casting process due to the influence of the cooling rate of the alloy melt during solidification. The A356 alloy belongs to a group of hypoeutectic Al–Si alloys (with 6.5–7.5 wt% silicon). According to the Al–Si phase diagram [11], solidification of this alloy begins with the formation of the α phase crystallites in the form of dendrites, in real casting conditions. The size of dendrites and the rate of dendritic growth depend on the cooling rate. The finest structure is obtained in the case of fast solidification (pressure casting). The structure of the eutecticum is important for the mechanical and tribological properties of the A356 alloy. The eutecticum of the A356 alloy consists of silicon needles or plates placed in the interdendritic space of the α phase [12]. Beside silicon, the presence of magnesium in the A356 alloy is also important for achieving good mechanical properties of the alloy. Because of the reactivity of magnesium, the intermetallic compound Mg_2Si is formed before the solidification of the alloy melt. The solubility of this compound in the lattice of α phase is limited. Therefore, heat treatment of the A356 alloy requires long solutionising and long-term artificial ageing. In addition, various intermetallic compounds can be formed in the alloy melt due to the presence of impurities (Cu, Mn, Fe, Ti, etc.). Some of these compounds have been identified in our previous study [9].

Under the influence of the shear forces during mixing of A356 alloy semi-solid melt (thixocasting process), the α phase particles have been transformed from dendritic to the non-dendritic form and elliptical α phase particles were formed. In the case of the applied mixing parameters [9], there was an increase in the α phase region in relation to the eutectic region, with an increase in size of α phase particles in the structure of the thixocasted A356 alloy. It was found that the structure of the A356 thixo alloy is coarsened compared to the structure of the cast A356 alloy [9]. Consequently, significantly less hardness of the A356 thixo alloy could be expected. However, the hardness values for the A356 thixo alloy (Table 1) and sand cast A356 alloy [1] are very close. This is probably due to the reduction in the porosity of the A356 thixo alloy during hot pressing, which was carried out in a solid state. The reduction in porosity is estimated on the basis of previously performed structural analysis [9]. Our other research [13] shows that the significantly higher hardness of the thixocasted A356 alloy was achieved after hot pressing in a semi-solid state, which resulted in better mechanical and tribological properties of the alloy.

After the incorporation of reinforcement (SiC) particles in the matrix alloy, a complex structure is formed, which affects the hardness of the composites. The presence of reinforcement particles leads to the matrix strengthening (mostly due to different coefficients of thermal expansion for ceramic particles and metal matrix, which shows a beneficial effect on composite hardness). However, an increase in the number of phase boundaries leads to an increase in the porosity of the composites. Also, the clusters of reinforcement particles have adverse effects on the composite hardness. These phenomena are more significant in hybrid composites (A356–10SiC–1Gr and A356–10SiC–3Gr), which leads to a greater dissipation of hardness values (Table 1).

Modulus of elasticity and shear modulus are mechanical properties that depend on the bond strength between the atoms in the material. Structure, heat treatment regime or cold plastic processing has little influence on these values [14]. As example, the hardness values are different for cast A356 alloys subjected to various heat treatments, while the modulus of elasticity and shear modulus are the same for all these cases [1]. Incorporation of SiC particles in the matrix alloy resulted in an increase in the values of the modulus of elasticity and shear modulus of the composite A356–10SiC, compared to the values of the A356 thixo alloy (Table 1) and the values of the cast A356 alloy [1]. This indicates a change in the nature of the material (composite A356–10SiC in relation to the matrix alloy), which led to an increase in the stiffness of the material. This means that a good bond between the SiC particles and the matrix has been achieved. Because of the addition of graphite particles, the modulus of elasticity and shear modulus of the hybrid composites (A356–10SiC–1Gr and A356–10SiC–3Gr) were reduced (Table 1), indicating that the stiffness of these hybrid composites is lower than the stiffness of the composite with ceramic reinforcements (A356–10SiC). With the increase in the amount of graphite particles, the modulus of elasticity and shear modulus values become lower due to the increase in the number of phase boundaries, which leads to an increase in the porosity of the composites.

3.2 Nanoscale properties

Microstructure of the tested materials was briefly analysed by using the OM images, since the detailed analysis of the materials microstructures is presented elsewhere [9]. Position of indents in each tested region of the α phase is denoted with arrow on OM images or with numbers on SPM images. In some cases, when nanoindentation was performed on intermetallic compounds or silicon particles in the α phase, very high values of nanohardness and modulus of elasticity were obtained. These values were not taken into account when analysing the nanoscale properties of the α phase, although they have influenced the overall macrohardness of the material to a certain extent. On the other hand, at some indents in the α phase regions, very low values of the nanohardness and modulus of elasticity were obtained. This is probably due to the presence of micropores in the material, so these results are also not taken into account when analysing the nanoscale properties of the tested materials.
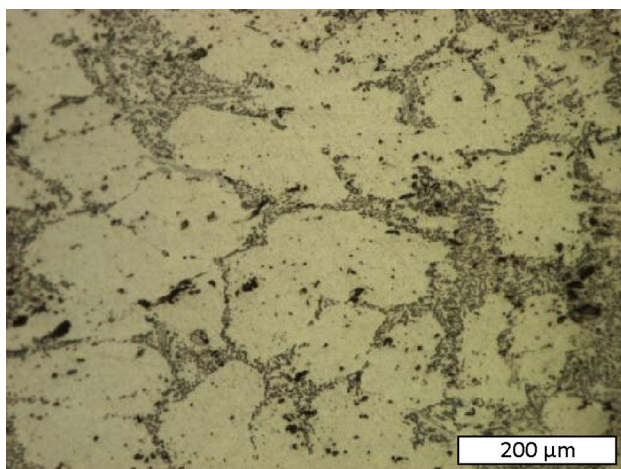
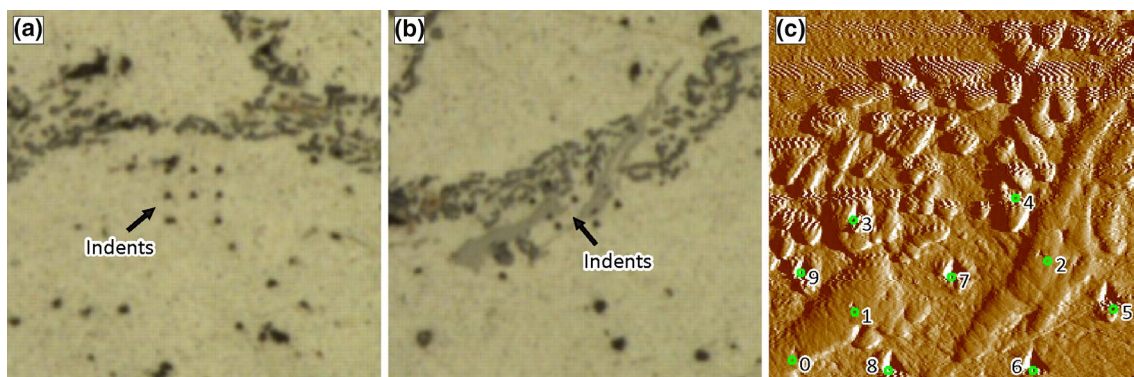**Fig. 3** Microstructure of A356 thixo alloy, OM image

3.2.1 A356 thixo alloy

Microstructure of A356 thixo alloy is shown in Fig. 3, where the eutectic areas can be seen between the elliptical regions of the α phase. Nanoindentation measurements of the A356 thixo alloy were performed on 2 different α phase regions, i.e. core of α phase and α phase in eutectic (eutectic α phase). Position of indents in the core of α phase region is shown in Fig. 4a. Seven of eight performed indents were selected to determine the nanoscale properties. The average value of nanohardness is 97.9 HV, while the average value of modulus of elasticity is 94.7 GPa.

Eutectic area with silicon particles in the form of nodules and irregular ellipses can be noticed in Fig. 4b. On a higher-magnification image (Fig. 4c), silicon particles can be seen as convex elements in relief, as well as particles of intermetallic compounds in the form of long irregular fibres. Position of indents in the eutectic α phase region is shown in Fig. 4b, c. Seven of ten performed indents were selected to determine the nanoscale properties. (Indents no. 0, 1 and 2 were not taken into account in averaging the values.) The average value of nanohardness is 110.1 HV, while the average value of modulus of elasticity is 102.5 GPa.

3.2.2 Composite A356–10SiC

Microstructure of composite A356–10SiC (Fig. 5) consists of the elliptical regions of α phase and eutectic areas. Most of the SiC particles are found in eutectic regions, along with silicon particles. Some of the SiC particles are in the cores of eutectic zones, while the other SiC particles are placed at α phase/eutecticum phase boundary. Nanoidentation measurements of the composite A356–10SiC were performed on 3 different α phase regions, i.e. core of α phase, α phase in eutectic (eutectic α phase) and α phase near SiC particles. Position of indents in the core of α phase region is also shown in Fig. 5. Six of nine performed indents were selected

Fig. 4 Position of indents in A356 thixo alloy: **a** core of α phase, OM (146×146 µm) image and **b, c** eutectic α phase, OM (146×146 µm) and SPM (40×40 µm) image
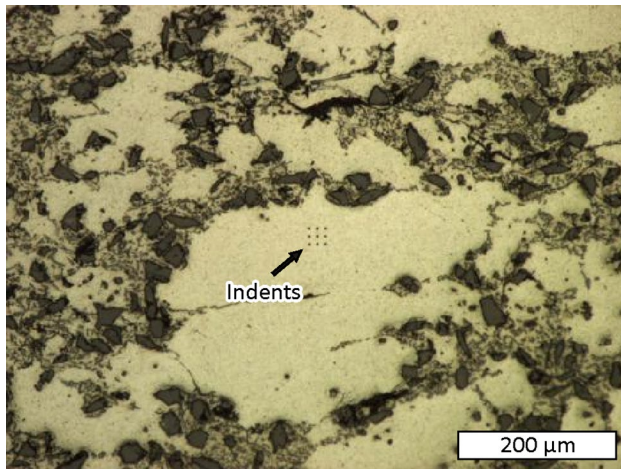
Fig. 5 Microstructure of composite A356–10SiC and position of indents in core of α phase, OM image

to determine the nanoscale properties. The average value of nanohardness is 88.6 HV, while the average value of modulus of elasticity is 82.3 GPa.

Eutectic area with silicon particles, SiC particles, α phase areas and position of indents in eutectic α phase is shown in Fig. 6a. Position of indents in the eutectic α phase region is more clearly visible on a higher-magnification image

(Fig. 6d). Four of eleven performed indents were selected to determine the nanoscale properties. (Indents no. 0, 1, 3, 4, 7, 9 and 10 were not taken into account in averaging the values.) The average value of nanohardness is 103.0 HV, while the average value of modulus of elasticity is 85.7 GPa.

Nanoidentation measurements of the α phase near SiC particle were performed in two areas, as shown in Fig. 6b, c. On both areas, the SiC particles were in the eutectic region. Position of indents in the α phase near SiC particle region is more clearly visible on higher-magnification images (Fig. 6e, i, f). All five indents were selected to determine the nanoscale properties. The average value of nanohardness is 89.3 HV, while the average value of modulus of elasticity is 85.4 GPa.

3.2.3 Hybrid composite A356–10SiC–1Gr

Microstructure of the hybrid composite A356–10SiC–1Gr is shown in Fig. 7. The regions of the α phase (bright fields) and eutectic regions with silicon particles and SiC particles can be seen, as well as some small graphite particles. Most of the SiC particles are found in eutectic regions, along with silicon particles. Nanoidentation measurements of the hybrid composite A356–10SiC–1Gr were performed on 5 different α phase regions, i.e. core of α phase, α phase in eutectic (eutectic α phase), α phase near SiC particles, α phase near
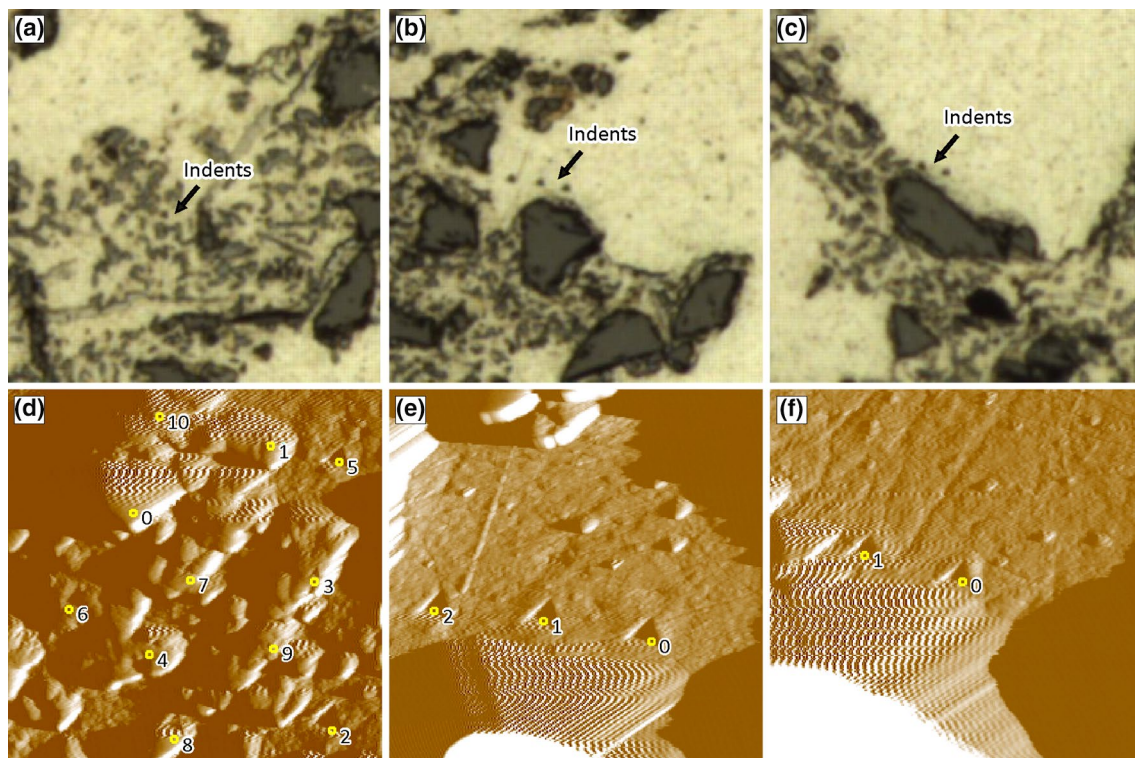
Fig. 6 Position of indents in composite A356–10SiC: **a**, **d** eutectic α phase, OM (146×146 μm) and SPM (40×40 μm) image and **b**, **c**, **e**, **f** α phase near SiC particle, OM (146×146 μm) and SPM (40×40 μm) images
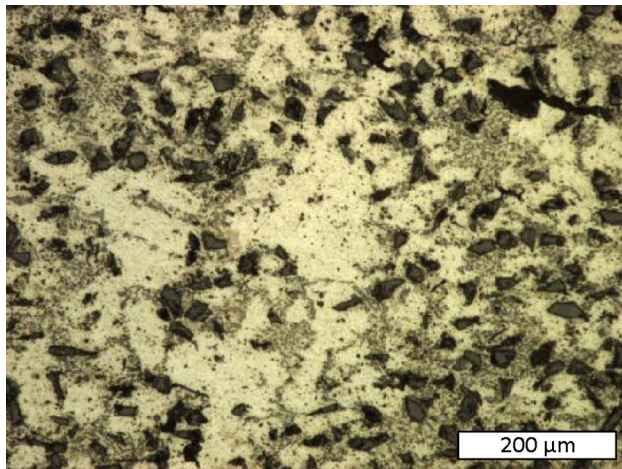
Fig. 7 Microstructure of hybrid composite A356–10SiC–1Gr, OM image

graphite particles and α phase near SiC and graphite particles. Position of indents in the core of α phase region is shown in Fig. 8a, b. Eight of nine performed indents were selected to determine the nanoscale properties. (Indent no. 4 was not taken into account in averaging the values.) The average value of nanohardness is 109.1 HV, while the average value of modulus of elasticity is 40.2 GPa.

Eutectic area with position of indents in eutectic α phase is shown on a higher-magnification image (Fig. 8c). Four of six performed indents were selected to determine the nanoscale properties. (Indents no. 0 and 4 were not taken into account in averaging the values.) The average value of nanohardness is 115.3 HV, while the average value of modulus of elasticity is 49.7 GPa.

Nanoidentation measurements of the α phase near SiC particle were performed in the eutectic region (α phase and silicon particles), as shown in Fig. 9a. Position of indents in the α phase near SiC particle region is more clearly visible

on a higher-magnification image (Fig. 9d). All five indents were selected to determine the nanoscale properties. The average value of nanohardness is 109.2 HV, while the average value of modulus of elasticity is 44.6 GPa.

Microstructure of the α phase near graphite particles region and position of performed indents is shown in Fig. 9b. A large graphite particle can be seen near the α phase. One part of this graphite particle is placed in the eutectic region. Position of indents in the α phase near graphite particle region is more clearly visible on a higher-magnification image (Fig. 9e). All three indents were selected to determine the nanoscale properties. The average value of nanohardness is 113.8 HV, while the average value of modulus of elasticity is 53.5 GPa.

Microstructure of the α phase near SiC and graphite particles region and position of performed indents is shown in Fig. 9c. In addition to one large particle of graphite, several SiC particles can be seen near the α phase. Position of indents in the α phase near SiC and graphite particle region is more clearly visible on a higher-magnification image (Fig. 9f). All four indents were selected to determine the nanoscale properties. The average value of nanohardness is 93.3 HV, while the average value of modulus of elasticity is 49.1 GPa.

3.2.4 Hybrid composite A356–10SiC–3Gr

Microstructure of hybrid composite A356–10SiC–3Gr is shown in Fig. 10. The regions of the α phase (bright fields) and eutectic regions with silicon particles and SiC particles can be seen, as well as part of one large graphite particles. Most of the SiC particles are found in eutectic regions, along with silicon particles. Nanoidentation measurements of the hybrid composite A356–10SiC–3Gr were also performed on 5 different α phase regions, i.e. core of α phase, α phase in eutectic (eutectic α phase), α phase near SiC particles, α phase near graphite particles and α
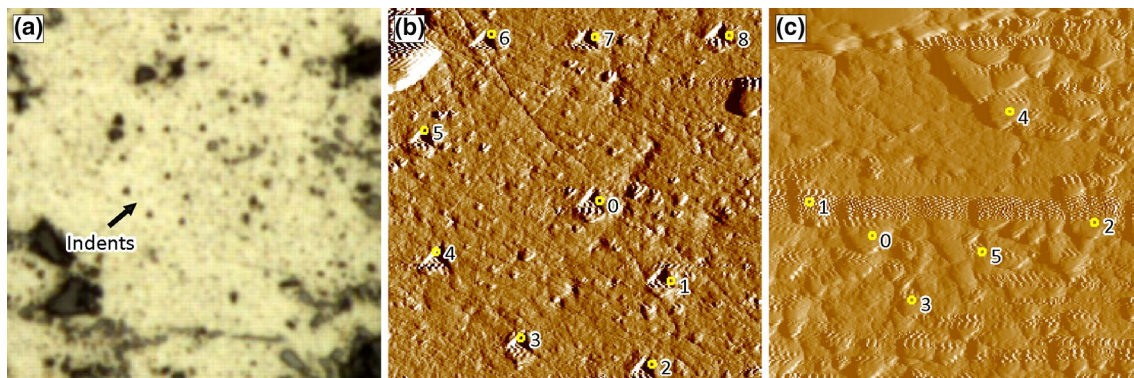
Fig. 8 Position of indents in hybrid composite A356–10SiC–1Gr: **a**, **b** core of α phase, OM (146×146 μm) and SPM (40×40 μm) image and **c** eutectic α phase, SPM (40×40 μm) image
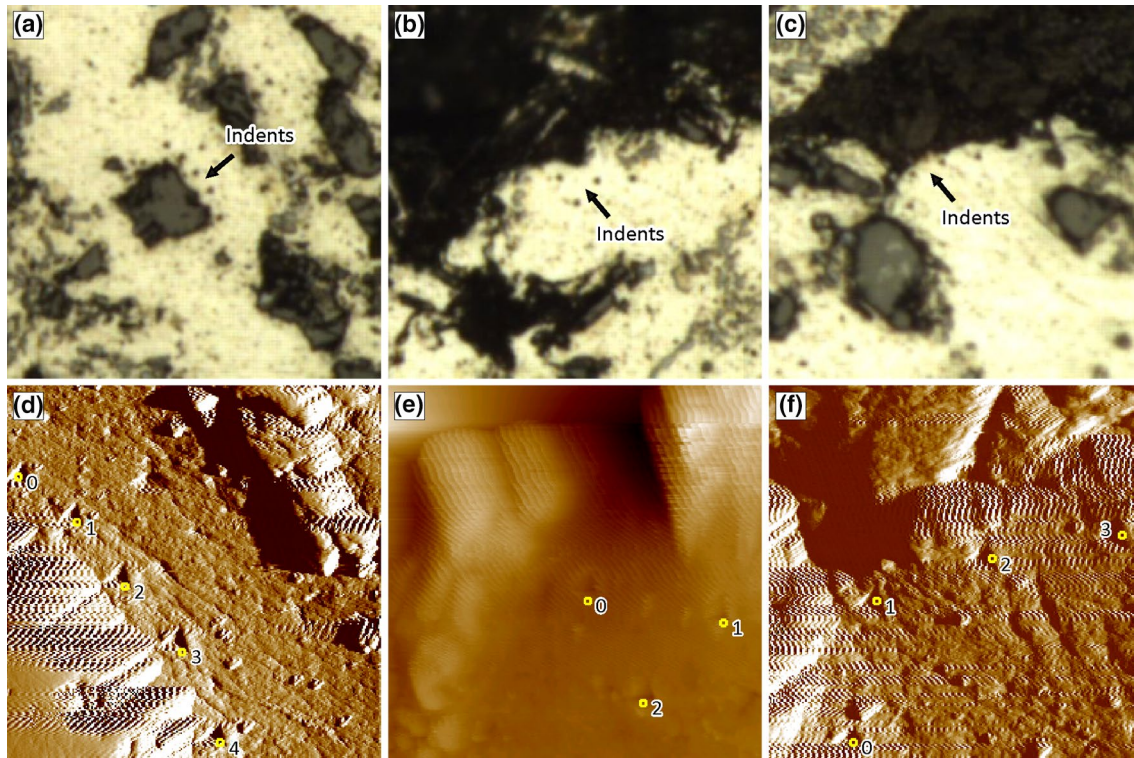
Fig. 9 Position of indents in hybrid composite A356–10SiC–1Gr: **a**, **d** α phase near SiC particle, OM (146×146 μm) and SPM (40×40 μm) image, **b**, **e** α phase near graphite particles, OM (146×146 μm) and SPM (40×40 μm) image and **c**, **f** α phase near SiC and graphite particles, OM (146×146 μm) and SPM (40×40 μm) image
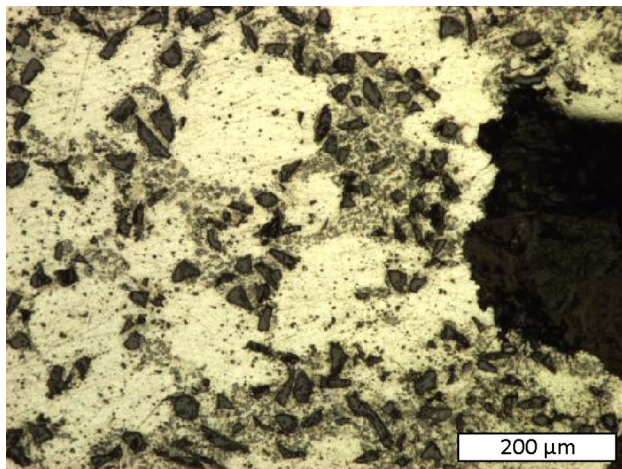
Fig. 10 Microstructure of hybrid composite A356–10SiC–3Gr, OM image

phase near SiC and graphite particles. Position of indents in the core of α phase region is shown in Fig. 11a. All nine indents were selected to determine the nanoscale properties. The average value of nanohardness is 98.6 HV, while the average value of modulus of elasticity is 26.6 GPa.

Eutectic area with silicon particles, SiC particles, α phase areas and position of indents in eutectic α phase is shown in Fig. 11b. Position of indents in the eutectic α phase region is more clearly visible on a higher-magnification image (Fig. 11c). Three of eight performed indents were selected to determine the nanoscale properties. (Indents no. 0, 2, 4, 5 and 7 were not taken into account in averaging the values.) The average value of nanohardness is 109.0 HV, while the average value of modulus of elasticity is 44.1 GPa.

Nanoidentation measurements of the α phase near SiC particle were performed in the eutectic region (α phase and silicon particles), as shown in Fig. 12a. Position of indents in the α phase near SiC particle region is more clearly visible on a higher-magnification image (Fig. 12d). Five of eight performed indents were selected to determine the nanoscale properties. (Indents no. 5, 6 and 7 were not taken into account in averaging the values.) The average value of nanohardness is 112.5 HV, while the average value of modulus of elasticity is 31.0 GPa.

Microstructure of the α phase near graphite particles region and position of performed indents is shown in Fig. 12b. A large graphite particle prevails on the image. Position of indents in the α phase near graphite particle region is more clearly visible on a higher-magnification image (Fig. 12e). All four indents were selected to determine
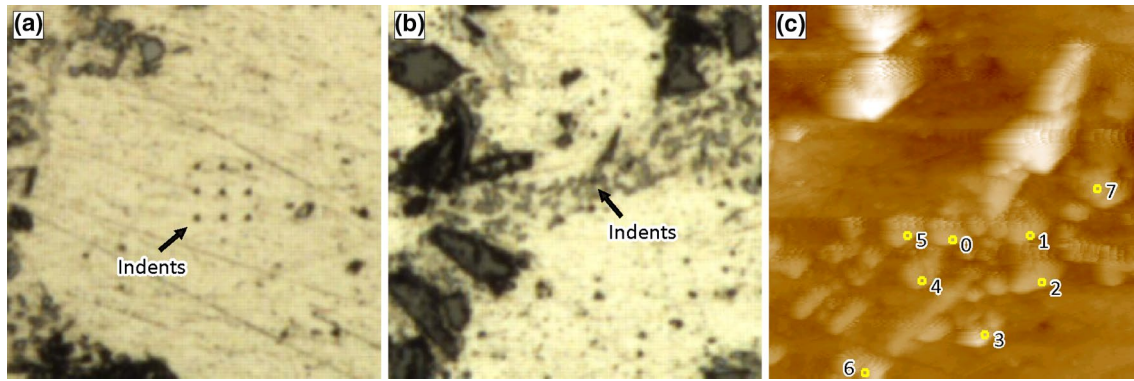
Fig. 11 Position of indents in hybrid composite A356–10SiC–3Gr: **a** core of α phase, OM (146×146 μm) and **b, c** eutectic α phase, OM (146×146 μm) and SPM (40×40 μm) image
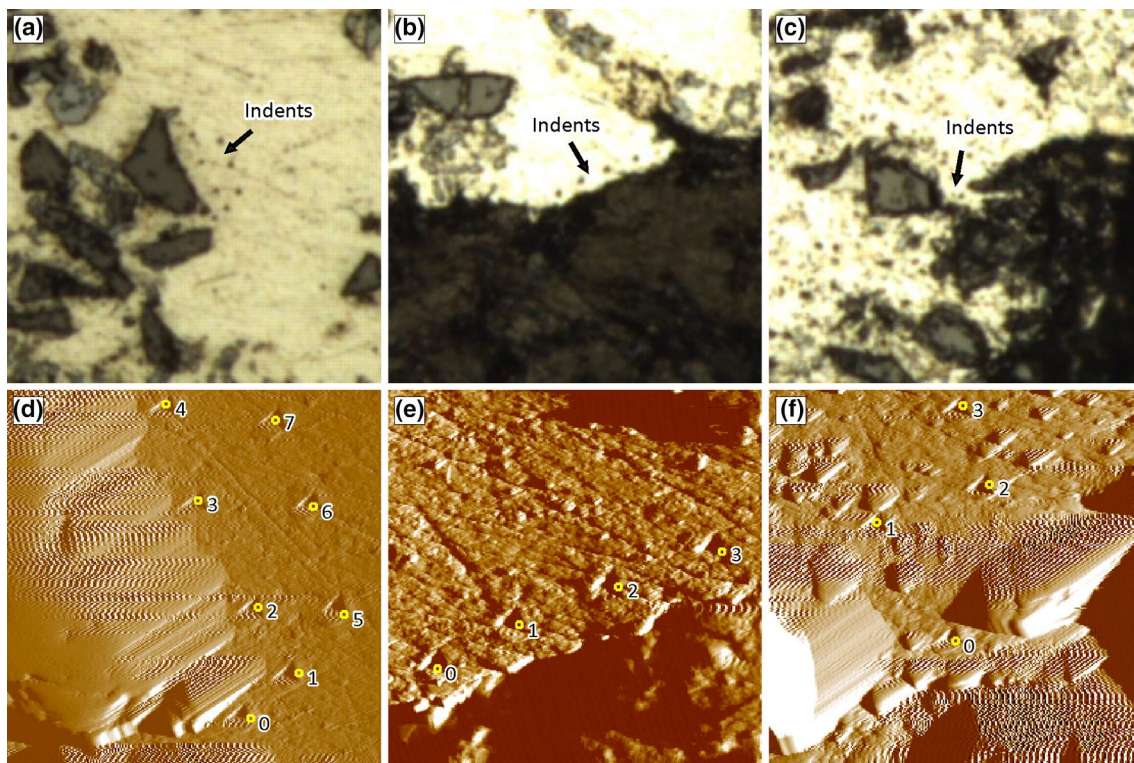
Fig. 12 Position of indents in hybrid composite A356–10SiC–3Gr: **a, d** α phase near SiC particle, OM (146×146 μm) and SPM (40×40 μm) image, **b, e** α phase near graphite particles, OM (146×146 μm) and SPM (40×40 μm) image and **c, f** α phase near SiC and graphite particles, OM (146×146 μm) and SPM (40×40 μm) image

the nanoscale properties. The average value of nanohardness is 110.0 HV, while the average value of modulus of elasticity is 42.5 GPa.

Microstructure of the α phase near SiC and graphite particles region and position of performed indents is shown in Fig. 12c. A narrow region of the α phase is placed between SiC particles and one large graphite particle. Position of indents in the α phase near SiC and graphite particle region is more clearly visible on a higher-magnification image (Fig. 12f). Three of four performed indents were selected to determine the nanoscale properties. (Indent no. 3 was not taken into account in averaging the values.) The average value of nanohardness is 97.5 HV, while the average value of modulus of elasticity is 27.0 GPa.

3.2.5 Discussion

Microstructure analysis of the A356 thixo alloy and the composites A356–10SiC, A356–10SiC–1Gr and A356–10SiC–3Gr (Figs. 3, 4, 5, 6, 7, 8, 9, 10, 11, 12) shows that silicon particles in all eutectic regions are compact, i.e. no broken silicon particles were detected at this level of examination. In composite materials, SiC particles are placed mainly in the eutectic regions, while the remaining SiC particles are visible near large elliptic (globular) particles of α phase. Large graphite particles are randomly distributed in the structure of hybrid composites. In our previous study [9], the presence of various intermetallic compounds in the eutectic regions was noticed, as well as the presence of individual silicon particles within the globules of α phase. In all composite materials, a good mechanical bond between the matrix and particles of secondary phases (SiC and graphite) was achieved. Phase boundaries matrix/secondary phases are continuous, without the presence of pores or dimples. Contact between particles of secondary phases was not observed.

The main microconstituent in the A356 alloy structure is the α phase (Al makes over 90 wt% of the alloy). Therefore, in order to make conclusions about the values of the basic mechanical properties at nanoscale, the nanoindentation measurements were performed on up to 5 different α phase regions on each material. Nanohardness and modulus of elasticity were measured in the core of α phase (within large globules of α phase), in the eutectic regions (where the area of α phase is significantly narrowed), and at the phase boundaries α phase/secondary phases (Figs. 3, 4, 5, 6, 7, 8, 9, 10, 11, 12). The obtained results were used to explain the influence of secondary phases on the values of the mechanical characteristics of the α phase. Nevertheless, it should be noted that the number of applied nanoindentations in different zones of the α phase is not sufficient for a comprehensive explanation of the different values of mechanical characteristics at nanoscale, neither in the case of the matrix A356

alloy nor in the case of produced composites. The obtained values of the nanohardness and modulus of elasticity depend on the type, size and content of the incorporated secondary phases, as well as on their position relative to the α phase. Variations in the values of mechanical properties of the composite materials are the result of a complex microstructure of the composites. For the purpose of easier comparison, values of nanohardness and modulus of elasticity of the different α phase regions in tested materials are summarised in two separate tables (Tables 2 and 3).

In the case of A356 thixo alloy, the average value of nanohardness in the eutectic α phase (α phase in the eutecticum) is higher than in the core of α phase (Table 2). A similar trend was observed in the case of the modulus of elasticity (Table 3). Higher values of the nanohardness and modulus of elasticity can be explained by the presence of silicon particles (which have higher strength than Al) in the eutecticum. The strengthening of α phase occurred near silicon particles, in the places where the nanoindentation measurements were performed. In the case of composite and hybrid composite materials, the addition of secondary phase (SiC and graphite) particles in the matrix also resulted in the strengthening of the matrix. However, due to the surface porosity of the secondary phase particles, pores can be entered into the phase boundary α phase (matrix)/particles, which reduces the effects of strengthening. In addition, the mixing of semi-solid composite melt lasted longer than the mixing of semi-solid melt of the A356 thixo alloy [9]. Since the mixing was carried out without a protective atmosphere, the entrapment of pores from the air was possible, although at this level of metallographic testing it was not noticed. These phenomena influenced the changes in the mechanical properties, especially at the phase boundaries α phase/secondary phases.

Microstructural analysis of the composite A356–10SiC showed that most of the SiC particles are placed in eutectic regions, along with silicon particles. A good mechanical bond was achieved between SiC particles and the metal matrix. The average values of nanohardness and modulus

Table 2 The average values of nanohardness of thixocasted A356 alloy and composites in the different α phase regions

Material designation	Nanohardness HV in appropriate α phase region				
	Core of α phase	α phase in eutectic	α phase near SiC_p	α phase near Gr_p	α phase near SiC_p and Gr_p
A356 thixo	97.9 (SD = 7.65)	110.1 (SD = 12.05)	–	–	–
A356–10SiC	88.6 (SD = 6.34)	103.0 (SD = 11.37)	89.3 (SD = 9.44)	–	–
A356–10SiC–1Gr	109.1 (SD = 6.66)	115.3 (SD = 11.71)	109.2 (SD = 9.36)	113.8 (SD = 4.21)	93.3 (SD = 1.12)
A356–10SiC–3Gr	98.6 (SD = 6.19)	109.0 (SD = 7.59)	112.5 (SD = 6.24)	110.0 (SD = 8.59)	97.5 (SD = 7.40)

SD: standard deviation

Table 3 The average values of modulus of elasticity of thixocasted A356 alloy and composites in the different α phase regions

Material designation	Modulus of elasticity, GPa in appropriate α phase region				
	Core of α phase	α phase in eutectic	α phase near SiC$_p$	α phase near Gr$_p$	α phase near SiC$_p$ and Gr$_p$
A356 thixo	94.7 (SD = 5.25)	102.5 (SD = 14.63)	–	–	–
A356–10SiC	82.3 (SD = 2.38)	85.7 (SD = 3.94)	85.4 (SD = 15.07)	–	–
A356–10SiC–1Gr	40.2 (SD = 1.75)	49.7 (SD = 5.83)	44.6 (SD = 1.75)	53.5 (SD = 1.21)	49.1 (SD = 0.73)
A356–10SiC–3Gr	26.6 (SD = 0.89)	44.1 (SD = 2.49)	31.0 (SD = 1.71)	42.5 (SD = 1.81)	27.0 (SD = 2.56)

SD: standard deviation

of elasticity in the eutectic α phase are higher than in the core of α phase (Tables 2 and 3). Due to the difference in coefficients of thermal expansion of the matrix and the reinforcement particles (literature data of the coefficients of thermal expansion are 21.5×10^{-6} m/mK for the A356 alloy and 4.3×10^{-6} m/mK for the SiC particles [15]), during cooling of the composite mixtures, there was an increase in dislocation density in the region near the reinforcements, which led to strengthening of the matrix [16]. The average values of nanohardness and modulus of elasticity in the α phase near SiC particles are higher than in the core of α phase, due to the effect of SiC particles. On the other hand, they are lower than in the eutectic α phase. This can be explained by the simultaneous influence of SiC and silicon particles on the mechanical properties of eutectic α phase, and by the possible presence of pores entered with the SiC particles.

In the case of hybrid composites A356–10SiC–1Gr and A356–10SiC3Gr, the analysis of the average values of nanohardness and modulus of elasticity shows that the presence of graphite particles resulted in their increase at the phase boundary α phase/graphite particles (α phase near graphite particles region) compared with the values in the core of α phase (Tables 2 and 3). They are very similar to the values measured in the eutectic α phase. These results are consistent with some literature data [17] and indicate the influence of graphite on the mechanical properties of hybrid composite matrix, due to the mismatch in the coefficients of linear thermal expansion of the matrix and graphite particles (21.5×10^{-6} m/mK for the matrix and $1.2–8.2 \times 10^{-6}$ m/mK for graphite [15]). On the other hand, the average values of nanohardness and modulus of elasticity become lower in the α phase near SiC and graphite particles regions, which can be expected in view of the possibility of introducing a greater amount of pores with the secondary phases particles. The average values of the modulus of elasticity of hybrid composites are lower than the modulus of elasticity of A356 thixo alloy and composite A356–10SiC, regardless of the region where the nanoindentation measurements were

performed. These results are, to some extent, consistent with the results obtained in macroscale characterisation (Table 1). The relatively low average values of the modulus of elasticity, obtained for hybrid composites in nanoscale measurements, indicate a weak bonding between the matrix (α phase) and graphite particles, at the level of atomic blocks.

4 Concluding remarks

The influence of secondary phases (SiC and graphite particles) in the A356 MMCs on their mechanical properties is analysed through the macro- and nanoscale measurements. Nanoscale measurements were performed on different α phase regions on each material (core of α phase, α phase in eutectic, α phase near SiC particles, α phase near graphite particles, and α phase near SiC and graphite particles). There is no direct correlation between mechanical properties on macro- and nanoscale.

The values of mechanical properties obtained at macroscale (macrohardness, modulus of elasticity and shear modulus) show that addition of SiC particles has beneficial influence on all tested mechanical properties, i.e. all of them are higher in composite containing only SiC particles than in the thixocast A356 alloy. The addition of large graphite particles together with SiC particles also has beneficial influence, since both hybrid composites have macrohardness higher than the composite containing only SiC particles. On the other hand, values of modulus of elasticity and shear modulus of hybrid composites (composites containing SiC and graphite particles) are reduced in relation to the composite containing only SiC particles. Hybrid composites with higher amount of graphite particles even have the lower values than thixocast A356 alloy. This indicates that the addition of large graphite particles leads to a reduction in stiffness in the material.

The values of mechanical properties obtained at nanoscale (nanohardness and modulus of elasticity in different α phase

regions) show that their values in the eutectic α phase are higher than in the core of α phase. This is explained with the presence of silicon particles in eutectic regions. The average values of nanohardness and modulus of elasticity in the α phase near SiC particles and in the α phase near graphite particles are also slightly higher than in the core of α phase. This strengthening is the result of an increase in the dislocation density near the phase boundaries due to the difference in the coefficients of thermal expansion between SiC or graphite particles and matrix. The full effect of secondary phase particles strengthening of the matrix is partially diminished by the possible presence of pores entered with those particles. The negative effect of porosity entered with secondary phase particles most probably prevailed in the regions of α phase near SiC and graphite particles. In these regions, mechanical properties are generally slightly lower than in the α phase near only one of the secondary phases.

The values of modulus of elasticity obtained at nanoscale for both hybrid composites are relatively low, regardless of the region where the measurements were performed. They are lower than the values of composite containing only SiC particles, as well as values of thixocast A356 alloy. This indicates that a good bond between the matrix (α phase) and graphite particles cannot be achieved at the atomic level.

References

1. Kearney AL (1990) (Rev.) Properties of cast aluminum alloys. In: ASM handbook, volume 2: properties and selection: nonferrous alloys and special-purpose materials. ASM International, Materials Park, pp 152–177
2. de Freitas E, Ferrante M, Ruckert CT, Bose Filho WW (2008) Thixocasting of an A356 alloy: fluidity, porosity distribution and thermomechanical fatigue behavior. Mater Sci Eng A 479(1–2):171–180
3. Möller H, Govender G, Stumpf WE (2010) Application of shortened heat treatment cycles on A356 automotive brake calipers with respective globular and dendritic microstructures. Trans Nonferrous Met Soc China 20(9):1780–1785
4. Vencl A (2012) Tribology of the Al–Si alloy based MMCs and their application in automotive industry. In: Magagnin L (ed) Engineered metal matrix composites: forming methods, material properties and industrial applications. Nova Science Publishers, New York, pp 127–166
5. Stojanović BŽ, Milojević ST (2017) Characterization, manufacturing and application of metal matrix composites. In: Wythers MC (ed) Advances in materials science research, vol 30. Nova Science Publishers, New York, pp 83–113
6. Flemings MC (1991) Behavior of metal alloys in the semisolid state. Metall Trans A 22(5):957–981
7. Yang JB, Lin CB, Wang TC, Chu HY (2004) The tribological characteristics of A356.2Al alloy/Gr$_{(p)}$ composites. Wear 257(9–10):941–952
8. Vencl A, Bobic I, Arostegui S, Bobic B, Marinković A, Babić M (2010) Structural, mechanical and tribological properties of A356 aluminium alloy reinforced with Al$_2$O$_3$, SiC and SiC + graphite particles. J Alloy Compd 506(2):631–639
9. Bobić I, Ružić J, Bobić B, Babić M, Vencl A, Mitrović S (2014) Microstructural characterization and artificial aging of compocasted hybrid A356/SiC$_p$/Gr$_p$ composites with graphite macroparticles. Mater Sci Eng A 612:7–15
10. Vencl A, Bobić I, Jovanović MT, Babić M, Mitrović S (2008) Microstructural and tribological properties of A356 Al–Si alloy reinforced with Al$_2$O$_3$ particles. Tribol Lett 32(3):159–170
11. Kearney A, Rooy EL (1990) (Rev.) Aluminum foundry products. In: ASM handbook volume 2: properties and selection: nonferrous alloys and special-purpose materials. ASM International, Metals Park, pp 123–151
12. Chalmers B (1964) Principles of solidification. Wiley, New York
13. Vencl A, Bobić I, Mišković Z (2008) Effect of thixocasting and heat treatment on the tribological properties of hypoeutectic Al–Si alloy. Wear 264(7–8):616–623
14. Dieter GE Jr (1963) Mechanical metallurgy. McGraw-Hill, New York
15. Alman DE (2001) Properties of metal–matrix composites. In: Miracle DB, Donaldson SL (eds) ASM handbook, volume 21: composites. ASM International, Materials Park, pp 838–858
16. Arsenault RJ, Wang L, Feng CR (1991) Strengthening of composites due to microstructural changes in the matrix. Acta Metall Mater 39(1):47–57
17. Wei JN, Cheng HF, Zhang YF, Han FS, Zhou ZC, Shui JP (2002) Effects of macroscopic graphite particulates on the damping behavior of commercially pure aluminum. Mater Sci Eng A 325(1–2):444–453